Biosensors and Bioelectronics 183 (2021) 113217

Contents lists available at ScienceDirect

Biosensors and Bioelectronics

journal homepage: http://www.elsevier.com/locate/bios

DNA-templated fluorescent silver nanoclusters on-off switch for specific and sensitive determination of organic mercury in seafood

Lin Huang [a], Peipei Li [a], Chen Lin [a], Yongning Wu [b], Zhiqiang Chen [a,**], FengFu Fu [a,*]

[a] Key Laboratory for Analytical Science of Food Safety and Biology of MOE, Fujian Provincial Key Lab of Analysis and Detection for Food Safety, College of Chemistry, Fuzhou University, Fuzhou, Fujian, 350116, China

[b] NHC Key Lab of Food Safety Risk Assessment, Food Safety Research Unit (2019RU014) of China Academy of Medical Science, China National Center for Food Safety Risk Assessment, Beijing, 100021, China

ARTICLE INFO

Keywords:
Mercury
AgNCs
Fluorescent biosensor
Seafood
Organic mercury

ABSTRACT

Organic mercury including methyl-mercury and ethyl-mercury (CH_3Hg^+ and $C_2H_5Hg^+$) has high toxicity and bio-accumulation, and thus is easy to generate bio-amplification in food chain. Hence, the specific detection of organic mercury has great significance for objectively assessing the health risk of mercury in seafood. We herein designed an aptamer ($A_{S\text{-}T7}$), which consists of a silver nanoclusters (AgNCs) scaffold sequence (A_S) and a T-rich sequence (A_{T7}), for simultaneously synthetizing DNA-templated AgNCs and recognizing organic mercury, and further developed a label-free fluorescent method for the sensitive and specific determination of organic mercury (CH_3Hg^+ and $C_2H_5Hg^+$ total concentration) by using DNA-templated AgNCs as signal. Without organic mercury, Ag^+ in the mixture of aptamer and Ag^+ was bond on A_S of aptamer to form A_S-templated AgNCs after reduction, and thus emitted strong fluorescence. Whereas, in the presence of organic mercury, $CH_3Hg^+/C_2H_5Hg^+$ was bond on A_{T7} of aptamer to generate photoinduced electron transfer (PET) between $CH_3Hg^+/C_2H_5Hg^+$ and A_S-templated AgNCs, and thus results in fluorescence quenching of A_S-templated AgNCs. The fluorescent method could be used to rapidly detect organic mercury with a detection limit of 5.0 nM (i.e. 1.01 ng Hg/g), which meets the U. S. EPA standard of 0.3 mg/kg (wet). The method was successfully used to detect organic mercury in water and fish muscle with a recovery of 96%–104% and an inter-days RSD ($n = 5$) < 7%. The success of the study promised a reliable method for rapid and specific detection of organic mercury in environmental and biological samples.

1. Introduction

In many developing countries, the coal consumption continues to grow rapidly due to the rapid development of economy, and thus results in a continuous increasing of mercury emitted into the global atmosphere (Pirrone et al., 2010; Yang et al., 2012). It was well known that mercury is a pervasive pollutant with high toxicity, and it can accumulate in organisms to cause irreversible damage to ecosystem and human health (Leopold et al., 2010; Morel et al., 1998). For above reasons, mercury and its compounds have been listed as priority hazardous substances by United Nations Environment Programme (UNEP) and United State Comprehensive Environmental Response, Compensation and Liability Act (CERCLA) (Pirrone et al., 2010). The inorganic mercury, mainly Hg^{2+}, released into aqueous and soil environments may be converted into more toxic organic mercury species, such as methyl-mercury (CH_3Hg^+) and ethyl-mercury ($C_2H_5Hg^+$), via biological and/or chemical processes (Kerin et al., 2006; Leopold et al., 2010; Poulain and Barkay, 2013).

Relative to inorganic and elemental mercury, organic mercury especially CH_3Hg^+ and $C_2H_5Hg^+$ has much stronger toxicity and high bio-accumulation, which easily generates bio-magnification of organic mercury concentration in food chain (Leopold et al., 2010; Mason et al., 1996). Therefore, marine organisms and seafood generally contained much higher organic mercury concentration than the ambient water they living. To ensure the consumption safety of seafood and human health, many countries and the World Health Organization (WHO) have established a much stricter limitation on the concentration of organic mercury in the aquatic environment and seafood than that of inorganic mercury (Hg^{2+}) (Leopold et al., 2010; Syversen and Kaur, 2012), and the determination of organic mercury has become mandatory in many

* Corresponding author.
** Corresponding author.
E-mail addresses: m171310007@fzu.edu.cn (Z. Chen), fengfu@fzu.edu.cn (F. Fu).

https://doi.org/10.1016/j.bios.2021.113217
Received 3 February 2021; Received in revised form 14 March 2021; Accepted 2 April 2021
Available online 6 April 2021
0956-5663/© 2021 Elsevier B.V. All rights reserved.

countries.

Currently, inductively coupled plasma mass spectrometry (ICP-MS)-based hyphenated techniques are mainly employed for the accurate determination of CH_3Hg^+ and $C_2H_5Hg^+$. For example, high performance liquid chromatography combined with ICP-MS (HPLC-ICP-MS) (Cairns et al., 2008; Zhu et al., 2017), ion chromatography coupled with ICP-MS (IC-ICP-MS) (Hong et al., 2011), gas chromatography coupled with ICP-MS (GC-ICP-MS) and capillary electrophoresis combined with ICP-MS (CE-ICP-MS) (Chen et al., 2016; Esteban-Fernández et al., 2012; Rahman et al., 2014; Zhao et al., 2012). Unfortunately, all above ICP-MS-based techniques not only required sophisticated and costly apparatus but also required the operator has professional skill, which makes the specific on-site determination of CH_3Hg^+ and $C_2H_5Hg^+$ in seafood impossible. Recently, a lot of sensors including chemsensors and DNA aptamer-based biosensors have been developed for the specific on-site detection of mercury (Chen et al., 2014a; Duan et al., 2014; Kim and Lee, 2018; Lee et al., 2009; Lou et al., 2011; Tan et al., 2016; Wen and Fan, 2017; Xie et al., 2010; Xue et al., 2008; Zhang et al., 2017), however, all these methods can be used for the detection of only Hg^{2+} and are incompetent for the rapid determination of CH_3Hg^+ and $C_2H_5Hg^+$. Lately, the techniques for the rapid and specific detection of organic mercury has made progress, some colorimetric and fluorescent methods have been developed for rapid detection of CH_3Hg^+ and/or $C_2H_5Hg^+$ based on functionalized nanomaterials or organic dye (Chen et al., 2014b, 2018, 2019; Costas-Mora et al., 2014; Deng et al., 2015; Zou and Tian, 2010). Unfortunately, colorimetric methods previously reported have lower sensitivity (Chen et al., 2014b, 2018, 2019), and the previous fluorescent methods suffered from one or more following defects such as poorer specificity, poor resistibility to complicated matrix, detection capability for only CH_3Hg^+, and higher cost due to the employment of dye-labeled DNA sequence (Costas-Mora et al., 2014; Deng et al., 2015; Zou and Tian, 2010).

Silver nanoclusters (AgNCs) have strong fluorescence emission ability due to the strong quantum-confinement effect (Guo et al., 2009). Particularly, DNA-scaffolded AgNCs was regarded as a promising fluorophores and has been widely used in fluorescent assay for the detection of inorganic ions, organic molecules, nucleic acids, virus and so on due to its low toxicity, excellent biocompatibility, tunable fluorescence emission and excellent stability (Han et al., 2019; Sharma et al., 2012; Shen et al., 2015; Yuan et al., 2014; Zhang et al., 2014, 2015; Zhang et al., 2014; Zou et al., 2019). On the other hand, it was reported that the T-rich DNA sequences can be used as probe for the recognition of different mercury species such as Hg^{2+} and organic mercury via elaborately designing the numbers and locations of T bases (Chen et al., 2018, 2019; Deng et al., 2015). In view of the properties of DNA-templated AgNCs and T-rich DNA sequences, we herein developed a label-free fluorescent AgNCs on-off switch for the rapid detection of organic mercury (total of CH_3Hg^+ and $C_2H_5Hg^+$) with high specificity and sensitivity by using DNA-templated AgNCs as signal and T-rich ssDNA sequences as the recognition probe, in order to provide a facile biosensor for on-site and cost-effective detection of organic mercury in aquatic environment and seafood to ensure the consumption safety of seafood.

2. Experimental section

2.1. Specific fluorescent detection of organic mercury (total of CH_3Hg^+ and $C_2H_5Hg^+$)

For detecting organic mercury (total of CH_3Hg^+ and $C_2H_5Hg^+$), firstly, 150 μL of 10 mM Tris-HNO_3 buffer (pH 7.0), 10 μL of CH_3Hg^+ or $C_2H_5Hg^+$ standard (or sample solution) and 10 μL of 15 μM DNA aptamer ($A_{S\text{-}T7}$, its sequences is: *ACC CGA ACC TGG GCT ACC ACC CTT AAT CCC C*GT TCT TTG TTA AAA ATT CTT TGT TCG G) solution was added and mixed in a centrifuge tube. Then, the mixture in the centrifuge tube was incubated for 1 h at 5 °C to obtain DNA-CH_3Hg^+ and/or DNA-$C_2H_5Hg^+$ conjugates. Subsequently, 10 μL of Ag^+ solution (0.12 mM) was added into the mixture and the whole was incubated for 20 min without light irradiation under room temperature. After added 10 μL of fresh $NaBH_4$ solution (0.24 mM, dissolved in cold water), the whole was gently mixed and then was incubated at 25 °C for 5 min in dark to produce DNA-templated AgNCs. The fluorescence emission spectra of the assay system were then measured with a microplate reader (Tecan Infinite M200 PRO) in the wavelength range of 550–750 nm at 520 nm excitation. The concentration of organic mercury was then quantified according to the fluorescence quenching ratio ($\Delta F/F_{(0)}$), where $\Delta F = F_{(0)} - F_{(+)}$, $F_{(0)}$ is the fluorescence intensity of the assay system at 620 nm without CH_3Hg^+ or $C_2H_5Hg^+$, and $F_{(+)}$ is the fluorescence intensity of the assay system at 620 nm in the presence of CH_3Hg^+ or $C_2H_5Hg^+$.

2.2. Determination of water and fish muscle sample

The tap water collected from our lab was directly filtered by a 0.22 μm filter membrane to remove any particulate matter, and EDTA with a final concentration of 20 μM was added to eliminate the interference of Cu^{2+}. Then, the organic mercury in the water sample was detected with the procedure described in 2.1.

To detect organic mercury in fish muscle sample (grouper) collected from Fujian of China. Firstly, each mercury species in 0.20 g of dried fish muscle was extracted out and further was concentrated to near dryness with previous method reported by Zhao et al. (2012) (details see Supporting Information, SI). The dryness of extract was then dissolved in 10.0 mL of Tris-HNO_3 buffer (pH 7.0) and a 20 μM final concentration of EDTA was added to eliminate the interference of Cu^{2+}. The organic mercury in final solution was then was detected according to process described in 2.1.

The water and fish muscle samples, which previously spiked with different CH_3Hg^+ and/or $C_2H_5Hg^+$ concentrations, were also determined with the same manner to obtain recovery.

3. Results and discussions

3.1. The principle for specific fluorescent detection of organic mercury based on DNA-templated AgNCs

As we mentioned above, an exquisitely-designed ssDNA sequence can be used as scaffold to synthetize DNA-templated AgNCs with good biocompatibility, excellent stability and higher quantum yields (Sharma et al., 2012), and an exquisitely-designed T-rich ssDNA sequence can be used as probe for specifically recognizing mercury species (Chen et al., 2018, 2019; Deng et al., 2015). Inspired by above findings, we herein designed a DNA aptamer ($A_{S\text{-}T7}$), which consists of a AgNCs scaffold sequence (Italic/blue part, called as A_S) and a T-rich sequence (underlined part, called as A_{T7}), for synthetizing DNA-templated AgNCs and specifically recognizing organic mercury (CH_3Hg^+ and $C_2H_5Hg^+$) at the same time, and further developed a label-free fluorescent method for rapid and sensitive detection of organic mercury by using A_S-templated AgNCs as signal molecules. As Scheme 1 showed, in the absence of CH_3Hg^+ and $C_2H_5Hg^+$, Ag^+ in the mixture of $A_{S\text{-}T7}$ aptamer and Ag^+ was bond on the A_S part of $A_{S\text{-}T7}$ under pH 7.0 and then to generate A_S-templated AgNCs, which emits strong fluorescence at 620 nm, after the associated Ag^+ was reduced by $NaBH_4$ (Sharma et al., 2012). Whereas, in the presence of CH_3Hg^+ or $C_2H_5Hg^+$, CH_3Hg^+ and $C_2H_5Hg^+$ can be bond on A_{T7} part of $A_{S\text{-}T7}$ since A_{T7} has stronger binding affinity to CH_3Hg^+ or $C_2H_5Hg^+$ over Hg^{2+} under pH 7.0 (Chen et al., 2018, 2019; Deng et al., 2015), and thus generates photoinduced electron transfer (PET) from A_S-templated AgNCs to $CH_3Hg^+/C_2H_5Hg^+$, which results in the fluorescence quenching of A_S-templated AgNCs. This provided a "turn-off" fluorescent platform for sensitive and specific detection of organic mercury.

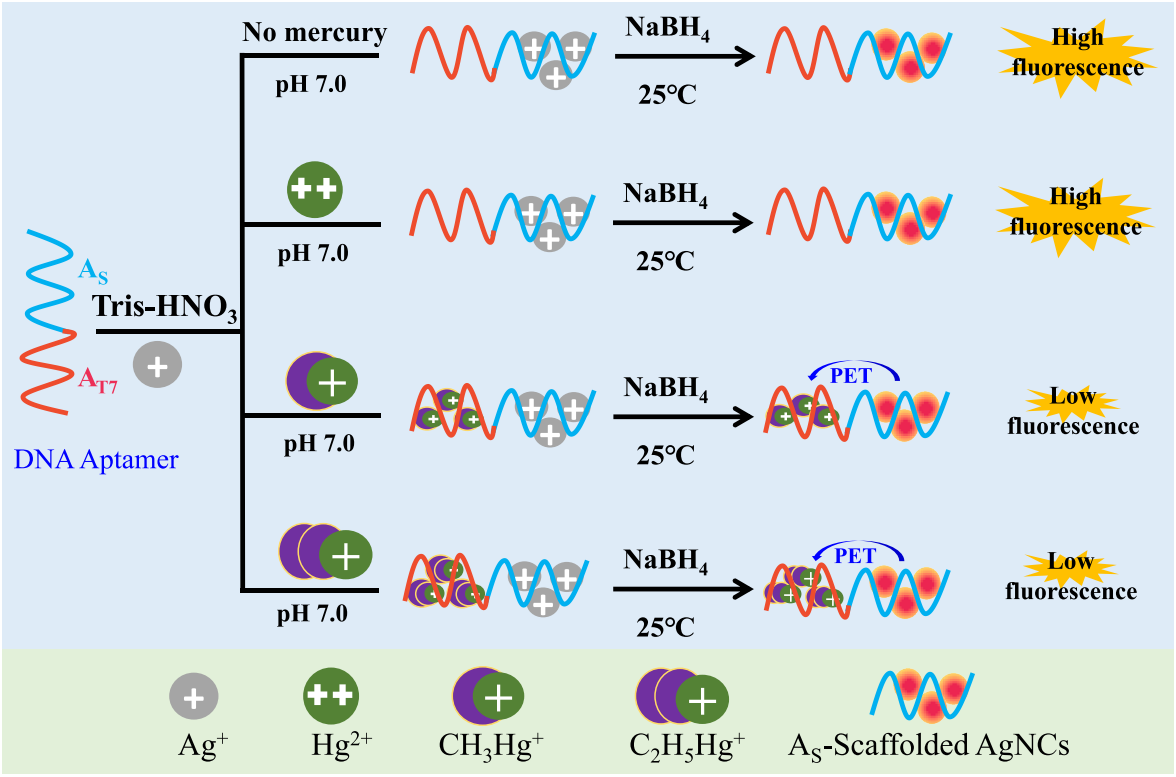

Scheme 1. Schematic diagram of the strategy for specific fluorescent detection of organic mercury based on DNA-templated AgNCs.

3.2. *Characterization of label-free A_S-templated AgNCs-based fluorescent biosensor*

To confirm the feasibility of our strategy, the fluorescence emission spectra of the assay system in the absence of mercury and in the presence of different mercury species was investigated in detail at 520 nm excitation. As Fig. 1 showed, in the case of no mercury species, the assay system emitted most strong fluorescence with a maximum emission wavelength at 620 nm, indicating that the A_S-templated AgNCs was successfully prepared in the presence of both $A_{S\text{-}T7}$ and Ag^+. The fluorescence quantum yield of the prepared A_S-templated AgNCs was measured with an Edinburgh FLS920 steady state and time resolved fluorescence spectrometer together with an integrating sphere by collecting the fluorescence from 500 to 760 nm, and the result showed the prepared A_S-templated AgNCs has a fluorescence quantum yield of ~28% (see Fig. S1 in SI), which is similar to that previously reported (Sharma 2012).

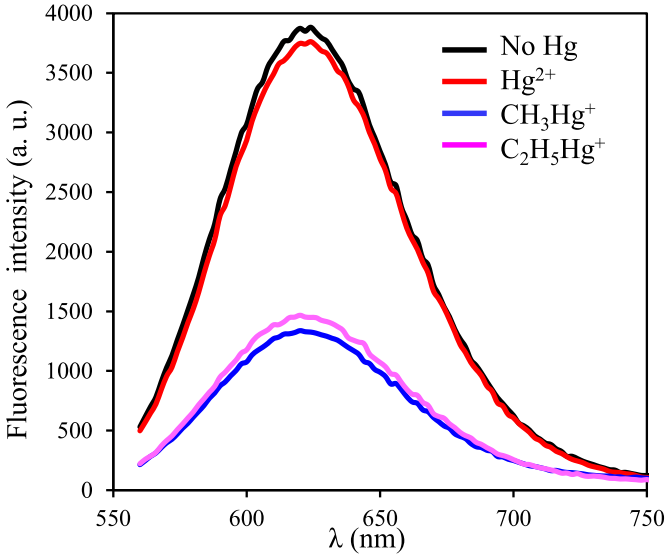

Fig. 1. Fluorescence emission spectra of the assay system in the absence of Hg species and in the presence of Hg^{2+}, CH_3Hg^+ and $C_2H_5Hg^+$. The excitation wavelength is 520 nm, and the concentrations of CH_3Hg^+, $C_2H_5Hg^+$ and Hg^{2+} are all 2.0 μM.

In the presence of inorganic mercury (Hg^{2+}), the fluorescence characteristics of the formed A_S-templated AgNCs keeps no change, indicating that no Hg^{2+} was bond on A_{T7} of $A_{S\text{-}T7}$ under pH 7.0 since if the Hg^{2+} was bond on A_{T7}, the A_{T7}-bond Hg^{2+} will be reduced by $NaBH_4$ to form Ag^0/Hg^0 amalgam nanoparticles and thus quench the fluorescence of A_S-templated AgNCs via fluorescence resonance energy transfer (FRET) (Deng et al., 2015). The image of transmission electron microscope (TEM) and the elemental analysis of energy dispersive X-ray spectrometry (EDX) shown in Fig. 2 further verified above deduction since no Hg signal was observed in EDX spectra (Fig. 2-B) in the case of Hg^{2+}.Whereas, upon the addition of CH_3Hg^+ or $C_2H_5Hg^+$, the fluorescence emission of the formed A_S-templated AgNCs significantly decreased (Fig. 1), indicating that CH_3Hg^+ or $C_2H_5Hg^+$ can effectively quench the fluorescence emission of A_S-templated AgNCs. To study the possible quenching mechanism by CH_3Hg^+ and $C_2H_5Hg^+$, the TEM images and the elemental analysis of EDX were first carried out. As Fig. 2-A showed, the AgNCs with a similar size of ~50 nm were observed in all cases in despite of the existence of mercury species or not. In addition, no matter whether mercury species were added or not, the formed A_S-templated AgNCs showed the same absorption spectra (see Fig. S2 in SI), which similar to that previously reported (Li and Wei, 2017). All above facts indicated that the addition of CH_3Hg^+ or $C_2H_5Hg^+$ do not affect the formation of A_S-templated AgNCs, which suggested that the fluorescence quenching of A_S-templated AgNCs by CH_3Hg^+ and $C_2H_5Hg^+$ is not caused by inter-particle aggregation. The absorption spectra of DNA-CH_3Hg^+ and DNA-$C_2H_5Hg^+$ conjugates showed no obvious absorption peak near 620 nm (Fig. S3 in SI), which is the

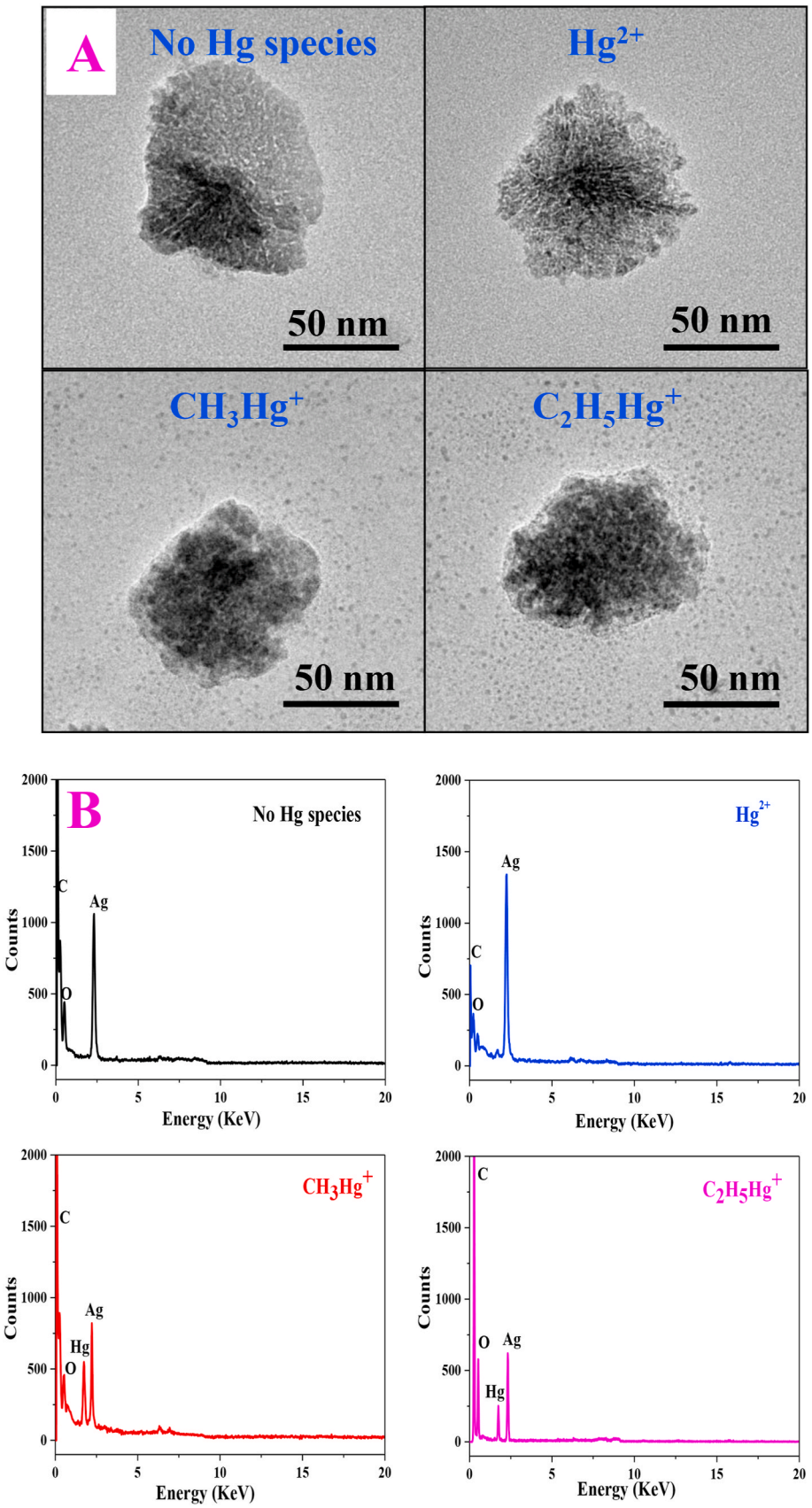

Fig. 2. TEM images (A) and EDX analysis (B) of the A_S-templated AgNCs observed in the assay system in the absence of Hg species and in the presence of Hg^{2+}, CH_3Hg^+ and $C_2H_5Hg^+$.

maximum emission wavelength of A_S-templated AgNCs, suggesting that the fluorescence quenching of A_S-templated AgNCs by CH_3Hg^+ and $C_2H_5Hg^+$ might also not be caused by fluorescence resonance energy transfer (FRET). By considering the facts that A_{T7} has much stronger binding affinity to CH_3Hg^+ or $C_2H_5Hg^+$ over Hg^{2+} under pH 7.0, which makes CH_3Hg^+ or $C_2H_5Hg^+$ can be rapidly bond on A_{T7} of $A_{S\text{-}T7}$ (Chen et al., 2018), and the redox potential of CH_3Hg^+ and $C_2H_5Hg^+$ is closed to the energy levels of DNA-templated AgNCs (0.089–0.103 eV) (Yuan et al., 2014). We deduced that the fluorescence quenching of A_S-templated AgNCs may be caused by the photoinduced electron transfer (PET) from A_S-templated AgNCs to $CH_3Hg^+/C_2H_5Hg^+$ (Zhang et al., 2014, 2014). An obvious Hg signal was observed in the EDX analysis of A_S-templated AgNCs in the case of CH_3Hg^+ and $C_2H_5Hg^+$ (Fig. 2-B) verified that CH_3Hg^+ and $C_2H_5Hg^+$ was really bond on A_{T7} end of $A_{S\text{-}T7}$ under pH 7.0.

3.3. Selection of DNA aptamer sequence

As we mentioned above, the DNA aptamer used in this study consisted of an AgNCs scaffold sequence (A_S) and a T-rich sequence (A_{T7}), which was used for synthetizing DNA-templated AgNCs and specifically recognizing $CH_3Hg^+/C_2H_5Hg^+$ respectively. It was well known, the binding affinity of T-rich DNA to different mercury species can be regulated by altering the number and location of T bases (Deng et al., 2015; Li et al., 2006). To realize the fluorescent detection of CH_3Hg^+ and $C_2H_5Hg^+$ with high specificity, three different ssDNA sequences ($A_{S\text{-}T5}$, $A_{S\text{-}T7}$ and $A_{S\text{-}T9}$), which contains different numbers of T bases (see Table S1 in SI), were designed by referring to previous study (Chen et al., 2018, 2019). As Fig. S4 (see SI) showed, among three DNA sequences, when $A_{S\text{-}T5}$ and $A_{S\text{-}T9}$ were used as DNA aptamer, all of Hg^{2+}, CH_3Hg^+ and $C_2H_5Hg^+$ can result in the fluorescence quenching of A_S-templated AgNCs with different sensitivity. That is, by using $A_{S\text{-}T5}$ and $A_{S\text{-}T9}$ as aptamer, the organic mercury could not be specifically detected. Whereas, by using $A_{S\text{-}T7}$ as aptamer, Hg^{2+} could not induce the fluorescence quenching of A_S-templated AgNCs, and only CH_3Hg^+ and $C_2H_5Hg^+$ could induced the fluorescence quenching of A_S-templated AgNCs with a similar sensitivity. That is, the organic mercury can be specifically detected with fluorescence spectrophotometry when $A_{S\text{-}T7}$ was used as aptamer. Thus, the $A_{S\text{-}T7}$ ssDNA was finally selected as the best aptamer sequence and was used in the next experiment.

3.4. Selection of other experimental conditions

The pH of the system directly affects the stability and redox potential of $NaBH_4$ solution, and finally affects the formation of A_S-templated AgNCs. As well, the pH of the system also affects the binding affinity of A_{T7} to different mercury species and thus affects the specificity of the method. As the results shown in Fig. S5 (see SI), the pH of the system had an obvious effect on the fluorescence intensity of the prepared A_S-templated AgNCs and the fluorescence quenching effect of mercury species. In the case of pH 6.5 and 7.5, the prepared A_S-templated AgNCs has a lower fluorescence emission, and all of Hg^{2+}, CH_3Hg^+ and $C_2H_5Hg^+$ can induce the fluorescence quenching with a different efficiency. When the pH was 7.9, the prepared A_S-templated AgNCs has a lowest fluorescence emission and all of Hg^{2+}, CH_3Hg^+ and $C_2H_5Hg^+$ induce the fluorescence quenching with a similar efficiency, indicating the designed aptamer has a similar binding affinity to Hg^{2+}, CH_3Hg^+ and $C_2H_5Hg^+$ under pH 7.9, like our previous report (Chen et al., 2018). Only under pH 7.0, the prepared A_S-templated AgNCs has a highest fluorescence emission, and CH_3Hg^+ and $C_2H_5Hg^+$ has a same and maximum fluorescence quenching effect. At the same time, Hg^{2+} does not induce fluorescence quenching. Above facts suggested that CH_3Hg^+ and $C_2H_5Hg^+$ can be specifically and sensitively detected under pH 7.0. Thus, pH 7.0 was selected as optimal pH in this study and was used in the next experiment.

The aptamer of $A_{S\text{-}T7}$ was used for synthetizing A_S-templated AgNCs and specifically recognizing $CH_3Hg^+/C_2H_5Hg^+$ simultaneously. The concentrations of $A_{S\text{-}T7}$ directly affect the preparation of A_S-templated AgNCs and thus affect the sensitivity of the method. To ascertain the best concentration of $A_{S\text{-}T7}$, the concentration of $A_{S\text{-}T7}$ was optimized in the range of 5.0 μM–20 μM under pH 7.0. The results revealed (Fig. S6 in SI) that a lower concentration of $A_{S\text{-}T7}$ do not provide adequate DNA template for synthetizing A_S-templated AgNCs to emit strong fluorescence and simultaneously provide adequate A_{T7} for completely binding $CH_3Hg^+/C_2H_5Hg^+$ to generate maximum fluorescence quenching, and thus results in a poor sensitivity and stability. When concentration of $A_{S\text{-}T7}$ is too high (20 μM), all of Hg^{2+}, CH_3Hg^+ and $C_2H_5Hg^+$ could induce fluorescence quenching with a different sensitivity since excess of $A_{S\text{-}T7}$ not only bind $CH_3Hg^+/C_2H_5Hg^+$ but also bind Hg^{2+}, and thus make CH_3Hg^+ and $C_2H_5Hg^+$ could not be specifically detected. When the concentration of $A_{S\text{-}T7}$ is 15 μM, the CH_3Hg^+ and $C_2H_5Hg^+$ could be specifically determined by fluorescent spectrometry with a similar and highest sensitivity. Thus, 15 μM of $A_{S\text{-}T7}$ was selected and used in the experiment.

The Ag^+ was used to synthetize AgNCs. Its concentration will directly affect the formation of A_S-templated AgNCs, and thus finally affect the analytical performance of the biosensor. The results showed in Fig. S7 (see SI) revealed, lower Ag^+ concentration could not provide adequate Ag^+ for the formation of A_S-templated AgNCs and thus lead to an extremely low fluorescence signal, whereas higher Ag^+ concentration prevented the effective formation of A_S-templated AgNCs and thus lead to an extremely low fluorescence signal or bad specificity too. When Ag^+ concentration is 0.12 mM, the as-prepared A_S-templated AgNCs has a maximum fluorescence emission, and simultaneously CH_3Hg^+ and $C_2H_5Hg^+$ could be specifically detected with a high sensitivity. Thus, 0.12 mM of Ag^+ was used in the experiment.

3.5. The specificity of the proposed method to organic mercury

There are many metallic ions coexisting in seafood and environmental samples, and these coexisting metallic ions might interfere with the detection of organic mercury. To evaluate the specificity of the proposed method, a variety of metallic ions including Na^+, K^+, Mg^{2+}, Zn^{2+}, Pb^{2+}, Ba^{2+}, Ca^{2+}, Ni^{2+}, Cu^{2+}, Al^{3+}, Fe^{3+} and Cr^{3+} with a 200 μM concentration, which is 100-fold that of mercury species (2.0 μM), were detected with the method. As Fig. 3-a revealed, only CH_3Hg^+ and $C_2H_5Hg^+$ can lead to a remarkable fluorescence quenching, and other metallic ions including Hg^{2+}, Na^+, K^+, Mg^{2+}, Zn^{2+}, Pb^{2+}, Ba^{2+}, Ca^{2+}, Ni^{2+}, Al^{3+}, Fe^{3+} and Cr^{3+} do not affect the fluorescence intensity of the assay system even if their concentrations are 100-fold of CH_3Hg^+ and $C_2H_5Hg^+$. However, 100-fold of Cu^{2+} obviously enhanced the fluorescence intensity of the assay system, and thus generates a positive interference with the detection of CH_3Hg^+ and $C_2H_5Hg^+$. To eliminate the positive interference of Cu^{2+}, we tried to add a 200 μM final concentration of EDTA in solution to chelate Cu^{2+}. As results shown in Fig. 3-b, upon the addition of EDTA, the positive interference of Cu^{2+} can be completely eliminated, whereas the $CH_3Hg^+/C_2H_5Hg^+$-induced fluorescence quenching was not affected since CH_3Hg^+ and $C_2H_5Hg^+$ is difficult to be chelated by EDTA. All above facts indicated that the proposed method has good selectivity, and can be used for the specific and sensitive detection of organic mercury.

3.6. The sensitivity and stability of label-free A_S-templated AgNCs-based fluorescent biosensor

Under above optimum experimental conditions, the fluorescence emission spectra of the assay system for detecting different concentrations of CH_3Hg^+ and $C_2H_5Hg^+$ (0.05 μM, 0.10 μM, 0.25 μM, 0.50 μM, 1.00 μM, 1.50 μM, 2.00 μM, 5.00 μM) were monitored, respectively. The results in Fig. 4 (a and b) showed, when CH_3Hg^+ and $C_2H_5Hg^+$ concentrations increased from 0.05 μM to 5.0 μM, the maximum fluorescence emission at 620 nm (F_{620}) decreased step by step. The fluorescence quenching ratio ($\Delta F/F_{(0)}$) of the assay system revealed a

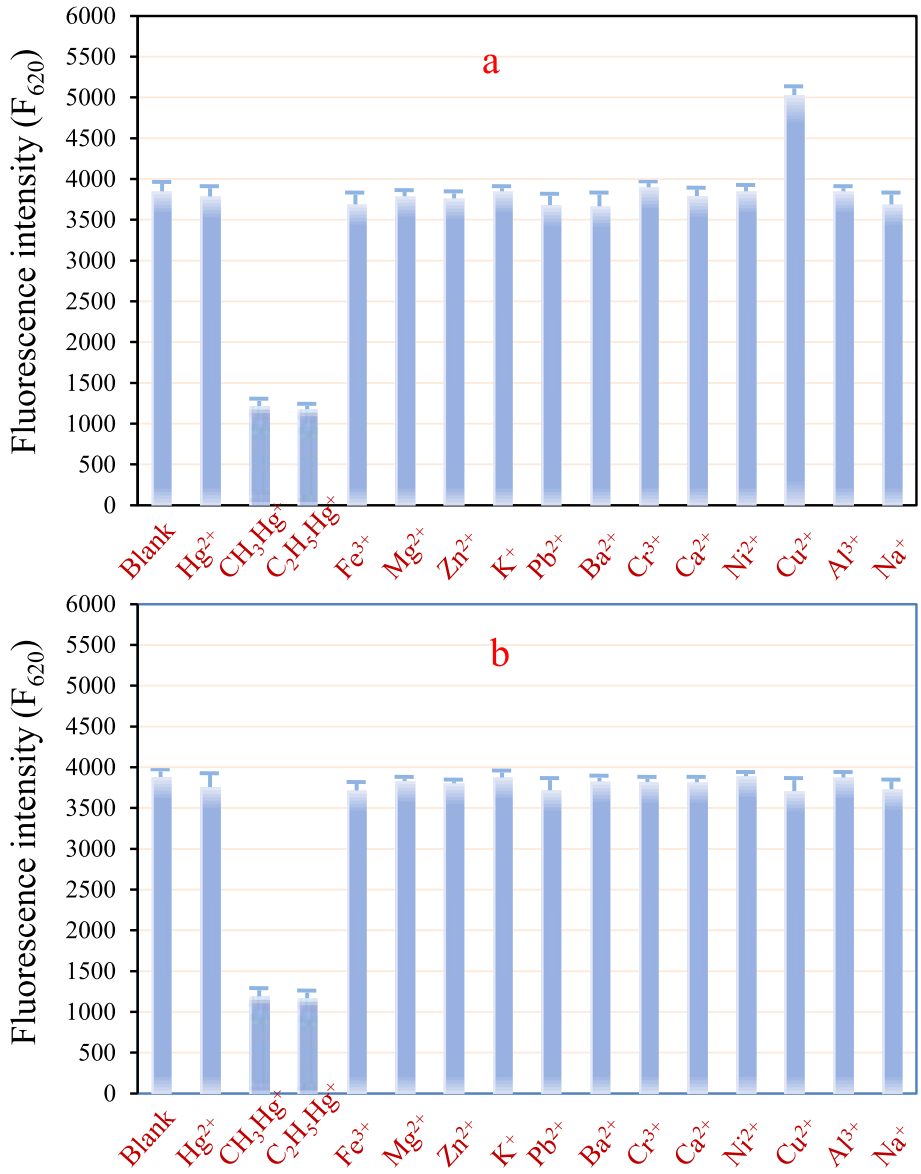

Fig. 3. The fluorescence intensity of the assay system for detecting various metallic ions under optimal conditions in the absence of EDTA (a) and in the presence of EDTA (b). The concentrations of Hg^{2+}, CH_3Hg^+ and $C_2H_5Hg^+$ are all 2.0 μM; the concentrations of other ions are all 200 μM.

good linear relationship with CH_3Hg^+ and $C_2H_5Hg^+$ concentrations within 0.05 μM–2.0 μM, with an equation of $\Delta F/F_{(0)} = 0.2357 \times C + 0.1889$ and $\Delta F/F_{(0)} = 0.2334 \times C + 0.1575$ for CH_3Hg^+ and $C_2H_5Hg^+$ respectively (C is the concentration of CH_3Hg^+ or $C_2H_5Hg^+$ with the unit of μM). Fig. 4 results clearly revealed that the developed method approximately has the same sensitivity for the detection of CH_3Hg^+ and $C_2H_5Hg^+$, and thus it could be used to detect the total concentration of CH_3Hg^+ and $C_2H_5Hg^+$, i.e., the concentration of organic mercury. The theoretical limit of detection (3σ/S) for both of CH_3Hg^+ and $C_2H_5Hg^+$ was calculated to be 5.0 nM (equivalent to 1.01 ng Hg/g), and the relative standard deviation (RSD) for the five repeated determinations of 1.0 μM CH_3Hg^+ or $C_2H_5Hg^+$ was calculated to be < 4%. In comparison with colorimetric methods and fluorescent methods previously reported, the proposed fluorescent method has higher or similar sensitivity (see Table S2 in SI) and meets the U.S. EPA standard of 0.3 mg/kg (wet) (Chen et al., 2018, 2019; Costas-Mora et al., 2014; Deng et al., 2015; Zou and Tian, 2010).

3.7. Determination of water and dried fish muscle sample

To verify the applicability and reliability of the developed method, the organic mercury in the tap water and fish muscle (grouper) collected from Fujian of China was detected with our method. The water and fish muscle samples previously spiked with different CH_3Hg^+ and/or $C_2H_5Hg^+$ concentrations were simultaneously detected with the same procedures to obtain recoveries. The obtained results were also compared with those detected with CE-ICP-MS, a reliable method for accurate analysis of CH_3Hg^+ and $C_2H_5Hg^+$. As Table 1 showed, the organic mercury in water and fish muscle samples can be specifically and sensitively detected with a recovery of 96%–104%, an intraday relative standard deviation (RSD, n = 5) < 6% and an inter-days RSD (n = 5) < 7%. The results obtained with the developed method consisted well with those detected with CE-ICP-MS. All above facts suggested that the developed fluorescent method has high sensitivity and good stability, and is reliable for the rapid and specific detection of organic mercury in seafood and water samples.

So far, the organic mercury in seafood and environmental samples were mainly detected by using ICP-MS-based hyphenated techniques

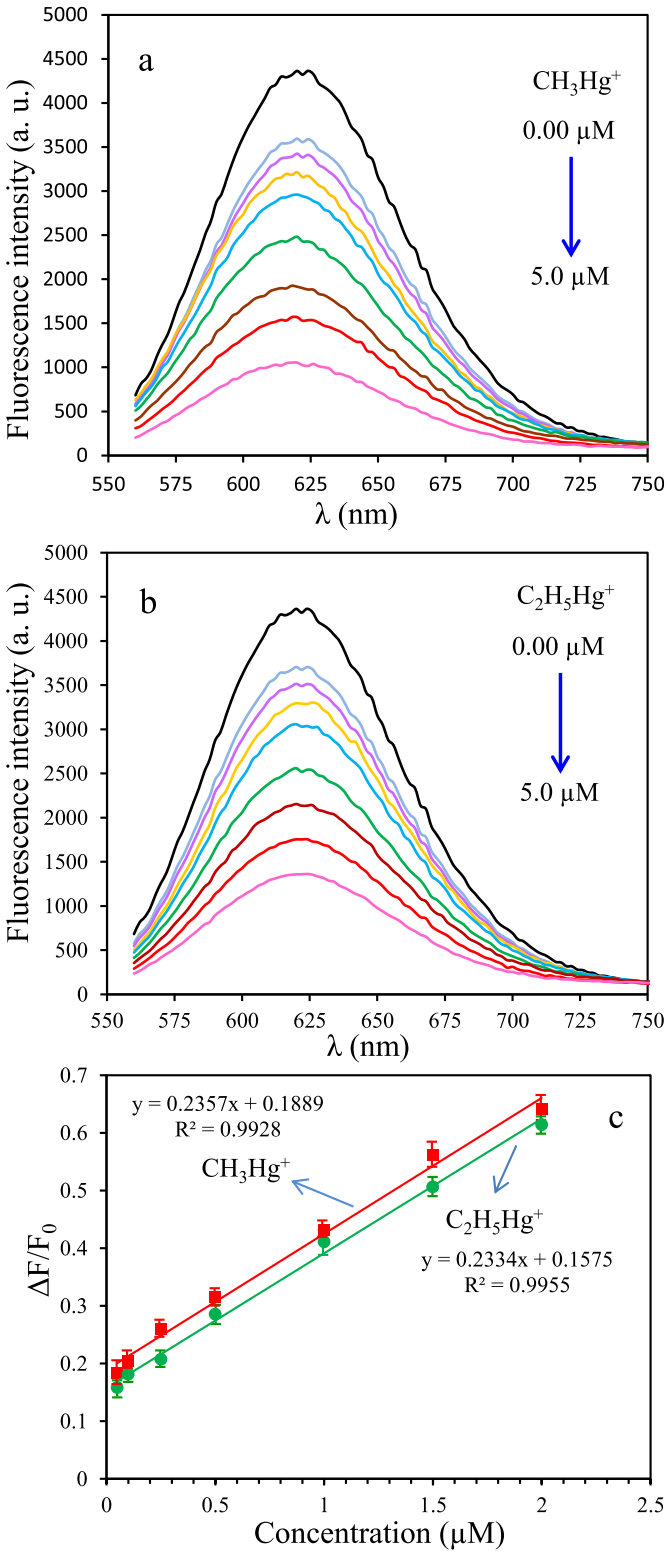

Fig. 4. The Fluorescence emission spectra of the assay system for detecting different concentrations of CH_3Hg^+ and $C_2H_5Hg^+$ (a, b), and the calibration curves for detecting CH_3Hg^+ and $C_2H_5Hg^+$ (c). The CH_3Hg^+ and $C_2H_5Hg^+$ concentrations are 0.00 μM, 0.05 μM, 0.10 μM, 0.25 μM, 0.50 μM, 1.00 μM, 1.50 μM, 2.00 μM and 5.00 μM.

(Cairns et al., 2008; Chen et al., 2016; Esteban-Fernandez et al., 2012; Hong et al., 2011; Rahman et al., 2014; Zhao et al., 2012; Zhu et al., 2017). However, the ICP-MS-based techniques required sophisticated and costly apparatus, long analysis time and skillful technician, which makes the specific on-site determination of CH_3Hg^+ and $C_2H_5Hg^+$ impossible. Although some colorimetric and fluorescent methods have been developed for rapid detection of CH_3Hg^+ and/or $C_2H_5Hg^+$ in recent (Chen et al., 2014b, 2018, 2019; Costas-Mora et al., 2014; Deng et al., 2015; Zou and Tian, 2010), the colorimetric methods previously reported have lower sensitivity and the previous fluorescent methods has poorer specificity and/or reproducibility, higher cost and only CH_3Hg^+ detection capability (see Table S2 in SI). The proposed fluorescent organic mercury biosensor has obvious analytical advantages such as label free, higher or similar sensitivity, lower cost, and detection capability for total of CH_3Hg^+ and $C_2H_5Hg^+$. All above features make our method a promising approach for the on-site detection of organic mercury in aqueous environment and seafood.

4. Conclusions

In summary, we herein fabricated a label-free fluorescent sensing platform for the specific and sensitive detection of organic mercury (total of CH_3Hg^+ and $C_2H_5Hg^+$) in aqueous environment and seafood based on DNA-templated AgNCs. We designed an aptamer ($A_{S\text{-}T7}$), which consists of an AgNCs scaffold sequence (A_S) and T-rich sequence (A_{T7}), for simultaneously synthetizing DNA-templated AgNCs and specifically recognizing organic mercury. Without organic mercury, Ag^+ in the mixture of aptamer and Ag^+ was bond on the A_S part of aptamer to form A_S-templated AgNCs after reduction, and then emitted strong fluorescence. Whereas, in the presence of organic mercury, $CH_3Hg^+/C_2H_5Hg^+$ can be bond on A_{T7} of aptamer to generate PET from A_S-templated AgNCs to $CH_3Hg^+/C_2H_5Hg^+$, and thus results in the fluorescence quenching of A_S-templated AgNCs. The method could be used to rapidly detect organic mercury with a detection limit of 5.0 nM (equivalent to 1.01 ng Hg/g), which meets the standard of 0.3 mg/kg (wet) defined by the U.S. EPA. The developed method has been successfully employed to detect organic mercury in water and fish muscle samples with a recovery of 96%–104%, an intraday RSD ($n = 5$) < 6% and an inter-days RSD ($n = 5$) < 7%. The success of the study promised a rapid and reliable method for on-site screening and detection of organic mercury in environmental and biological samples.

CRediT authorship contribution statement

Lin Huang: Writing – original draft, performed the experiments. The manuscript was written through contributions of all authors, and all authors have given approval to the final version of the manuscript. **Peipei Li:** Writing – original draft, performed the experiments. The manuscript was written through contributions of all authors, and all authors have given approval to the final version of the manuscript. **Chen Lin:** Writing – original draft, performed the experiments. The manuscript was written through contributions of all authors, and all authors have given approval to the final version of the manuscript. **Yongning Wu:** Data curation, Formal analysis, Writing – original draft, co-performed data analysis and interpretation. The manuscript was written through contributions of all authors, and all authors have given approval to the final version of the manuscript. **Zhiqiang Chen:** Data curation, Formal analysis, Writing – original draft, performed the experimental design, data analysis and interpretation, and manuscript writing. The manuscript was written through contributions of all authors, and all authors have given approval to the final version of the manuscript. **FengFu Fu:** Data curation, Formal analysis, Writing – original draft, Chen performed the experimental design, data analysis and interpretation, and manuscript writing. The manuscript was written through contributions of all authors, and all authors have given approval to the final version of the manuscript.

Table 1
Analytical results of organic mercury in water and dried fish muscle samples.

Sample		Added CH_3Hg^+ (μM)	Added $C_2H_5Hg^+$ (μM)	[b]Detection of total CH_3Hg^+ and $C_2H_5Hg^+$				[c]CE-ICP-MS	
				Con. (μM)	Rec.	Intraday RSD (n = 5)	Inter-days RSD (n = 5)	CH_3Hg^+ (μM)	$C_2H_5Hg^+$ (μM)
Tap water	1	0.00	0.00	–	–	–	–	–	–
	2	0.50	0.00	0.48	96%	5%	6%	0.51	0.0
	3	0.00	0.50	0.52	104%	3%	5%	0.0	0.49
	4	0.25	0.25	0.49	98%	5%	6%	0.24	0.25
[a]Fish muscle	5	0.00	0.00	0.19	–	6%	7%	0.20	0.0
	6	0.50	0.00	0.70	102%	3%	5%	0.69	0.0
	7	0.00	0.50	0.71	104%	4%	5%	0.21	0.51
	8	0.25	0.25	0.68	98%	5%	6%	0.46	0.26

[a] The concentration in the 10 mL extract of 0.20 g dried fish muscle.
[b] The data obtained with our method.
[c] The data obtained with CE-ICP-MS method reported in Zhao et al. (2012).

Declaration of competing interest

The authors declare that they have no known competing financial interests or personal relationships that could have appeared to influence the work reported in this paper.

Acknowledgements

The authors gratefully acknowledge The National Key Research and Development Program of China (2017YFC1600500), NSFC (21976029) and Fujian Provincial Department of Science and Technology (2019Y0002) for financial support.

Appendix A. Supplementary data

Supplementary data to this article can be found online at https://doi.org/10.1016/j.bios.2021.113217.

References

Cairns, W.R.L., Ranaldo, M., Hennebelle, R., Turetta, C., Capodaglio, G., Ferrari, C.F., Dommergue, A., Cescon, P., Barbante, C., 2008. Anal. Chim. Acta 622, 62–69.
Chen, G.H., Chen, W.Y., Yen, Y.C., Wang, C.W., Chang, H.T., Chen, C.F., 2014a. Anal. Chem. 86, 6843–6849.
Chen, L., Li, J.H., Chen, L.X., 2014b. ACS Appl. Mater. Interfaces 6, 15897–15904.
Chen, Y.Q., Cheng, X., Mo, F., Huang, L.M., Wu, Z.J., Wu, Y.N., Xu, L.J., Fu, F.F., 2016. Electrophoresis 37, 1055–1062.
Chen, Z.Q., Li, P.P., Cheng, X., Yang, W.J., Wu, Y.N., Chen, Q.A., Fu, F.F., 2019. ACS Omega 4, 15112–15119.
Chen, Z.Q., Wang, X.S., Cheng, X., Yang, W.J., Wu, Y.N., Fu, F.F., 2018. Anal. Chem. 90, 5489–5495.
Costas-Mora, I., Romero, V., Lavilla, I., Bendicho, C., 2014. Anal. Chem. 86, 4536–4543.
Deng, L., Li, Y., Yan, X.P., Xiao, J., Ma, C., Zheng, J., Liu, S.J., Yang, R.H., 2015. Anal. Chem. 87, 2452–2458.
Duan, J.L., Yin, H.Z., Wei, R.R., Wang, W.W., 2014. Biosens. Bioelectron. 57, 139–142.
Esteban-Fernández, D., Mirat, M., Ignacia Martín de la Hinojosa, M., Ignacio Gar-cía Alonso, J., 2012. J. Agric. Food Chem. 60, 8333–8339.
Guo, W.W., Yuan, J.P., Wang, E.K., 2009. Chem. Commun. 23, 3395–3397.
Han, Y.P., Zhang, F., Gong, H., Cai, C.Q., 2019. Anal. Chim. Acta 1053, 105–113.
Hong, Y.S., Rifkin, E., Bouwer, E.J., 2011. Environ. Sci. Technol. 45, 6429–6436.
Kerin, E.J., Gilmour, C.C., Roden, E., Suzuki, M.T., Coates, J.D., Mason, R.P., 2006. Appl. Environ. Microbiol. 72, 7919–7921.
Kim, H.J., Lee, H.I., 2018. ACS Appl. Mater. Interfaces 10, 34634–34639.
Lee, J., Jun, H., Kim, J., 2009. Adv. Mater. 21, 3674–3677.
Leopold, K., Foulkes, M., Worsfold, P., 2010. Anal. Chim. Acta 663, 127–138.
Li, C.Y., Wei, C.Y., 2017. Sensor. Actuator. B Chem. 242, 563–568.
Li, Y., Jiang, Y., Yan, X.P., 2006. Anal. Chem. 78, 6115–6120.
Lou, T.T., Chen, Z.P., Wang, Y.Q., Chen, L.X., 2011. ACS Appl. Mater. Interfaces 3, 1568–1573.
Mason, R.P., Reinfelder, J.R., Morel, F.M.M., 1996. Environ. Sci. Technol. 30, 1835–1845.
Morel, F.M.M., Kraepiel, A.M.L., Amyot, M., 1998. Annu. Rev. Ecol. Systemat. 29, 543–566.
Pirrone, N., Cinnirella, S., Feng, X., Finkelman, R.B., Friedli, H.R., Leaner, J., Mason, R., Mukherjee, A.B., Stracher, G.B., Streets, D.G., Telmer, K., 2010. Atmos. Chem. Phys. 10, 5951–5964.
Poulain, A., Barkay, T., 2013. Science 339, 1280–1281.
Rahman, G.M.M., Wolle, M.M., Fahrenholz, T., Kingston, H.M.S., Pamuku, M., 2014. Anal. Chem. 86, 6130–6137.
Sharma, J., Rocha, R.C., Phipps, M.L., Yeh, H.C., Balatsky, K.A., Vu, D.M., Shreve, A.P., Werner, J.H., Martinez, J.S., 2012. Nanoscale 4, 4107–4110.
Shen, C.C., Xia, X.D., Hu, S.Q., Yang, M.H., Wang, J.X., 2015. Anal. Chem. 87, 693–698.
Syversen, T., Kaur, P., 2012. J. Trace Elem. Med. Biol. 26, 215–226.
Tan, F., Cong, L.C., Saucedo, N.M., Gao, J.S., Li, X.N., Mulchandani, A., 2016. J. Hazard Mater. 320, 226–233.
Wen, X.Y., Fan, Z.F., 2017. Sensor. Actuator. B Chem. 247, 655–663.
Xie, J.P., Zheng, Y.G., Ying, J.Y., 2010. Chem. Commun. 46, 961–963.
Xue, X., Wang, F., Liu, X., 2008. J. Am. Chem. Soc. 130, 3244–3245.
Yang, Y.F., Huang, Q.F., Wang, Q., 2012. Environ. Sci. Technol. 46, 3058–3059.
Yuan, Z., Chen, Y.C., Li, H.W., Chang, H.T., 2014. Chem. Commun. 50, 9800–9815.
Zhang, K., Wang, K., Zhu, X., Zhang, J., Xu, L., Huang, B., Xie, M.H., 2014a. Chem. Commun. 50, 180–182.
Zhang, S.T., Zhang, D.X., Zhang, X.H., Shang, D.H., Xue, Z.H., Shan, D.L., Lu, X.Q., 2017. Anal. Chem. 89, 3538–3544.
Zhang, S.W., Li, J.X., Zeng, M.Y., Xu, J.Z., Wang, X.K., Hu, W.P., 2014b. Nanoscale 6, 4157–4162.
Zhang, Y., Zhu, C.F., Zhang, L., Tan, C.L., Yang, J., Chen, B., Wang, L.H., Zhang, H., 2015. Small 11, 1385–1389.
Zhao, Y.Q., Zheng, J.P., Fang, L., Lin, Q., Wu, Y.N., Xue, Z.M., Fu, F.F., 2012. Talanta 89, 280–285.
Zhu, S.Q., Chen, B.B., He, M., Huang, T., Hu, B., 2017. Talanta 171, 213–219.
Zou, Q., Tian, H., 2010. Sensor. Actuator. B Chem. 149, 20–27.
Zou, R., Zhang, F., Chen, C.Y., Cai, C.Q., 2019. Sensor. Actuator. B Chem. 296, 126608.